CrossMark

Rainfall variability and trends of the past six decades (1950–2014) in the subtropical NW Argentine Andes

F. Castino[1] · B. Bookhagen[1] · M. R. Strecker[1]

Abstract The eastern flanks of the Central Andes are characterized by deep convection, exposing them to hydrometeorological extreme events, often resulting in floods and a variety of mass movements. We assessed the spatiotemporal pattern of rainfall trends and the changes in the magnitude and frequency of extreme events ($\geq$95th percentile) along an E-W traverse across the southern Central Andes using rain-gauge and high-resolution gridded datasets (CPC-uni and TRMM 3B42 V7). We generated different climate indices and made three key observations: (1) an increase of the annual rainfall has occurred at the transition between low (<0.5 km) and intermediate (0.5–3 km) elevations between 1950 and 2014. Also, rainfall increases during the wet season and, to a lesser degree, decreases during the dry season. Increasing trends in annual total amounts characterize the period 1979–2014 in the arid, high-elevation southern Andean Plateau, whereas trend reversals with decreasing annual total amounts were found at low elevations. (2) For all analyzed periods, we observed small or no changes in the median values of the rainfall-frequency distribution, but significant trends with intensification or attenuation in the 95th percentile. (3) In the southern Andean Plateau, extreme rainfall events exhibit trends towards increasing magnitude and, to a lesser degree, frequency during the wet season, at least since 1979. Our analysis revealed that low (<0.5 km), intermediate (0.5–3 km), and high-elevation (>3 km) areas respond differently to changing climate conditions, and the transition zone between low and intermediate elevations is characterized by the most significant changes.

1 Introduction

Extreme hydrometeorological events are important drivers for a variety of natural hazards, including floods, landslides, and other mass movements (White and Haas 1975; Caine 1980), often associated with severe damages and high costs. In light of a suspected worldwide increase of such events, it has been argued that this trend may be a result of global warming (e.g., Trenberth et al. 2003; Seneviratne et al. 2012). Several studies have shown an increasing magnitude and/or frequency in extreme rainfall events in a wide variety of environments (e.g., Haylock and Nicholls 2000; Goswami et al. 2006; Malik et al. 2011). This is partly in agreement with predictions and future climate projections in the context of continued global change (e.g., Trenberth et al. 2003; Giorgi and Lionello 2008).

High-elevation regions are particularly sensitive to the effects of global warming and are considered the sentinels of climate change, since they are thought to respond rapidly and intensely to changing environmental conditions (e.g., Beniston et al. 1996; Pepin et al. 2015; Vuille et al. 2015). Several synoptic-scale studies have addressed changes of rainfall extremes in areas including mountain ranges, such as the Himalaya and the Andes, from which fundamental impacts on the landscape and the human habitat can

✉ F. Castino
castino@geo.uni-potsdam.de

1 Institute of Earth- and Environmental Sciences, University of Potsdam, Potsdam, Germany

🖄 Springer

be expected (Marengo 2004; Penalba and Robledo 2010; Espinoza et al. 2012; Barros et al. 2013; Skansi et al. 2013; Robledo et al. 2015; Malik et al. 2016). However, these studies are generally limited to station data recorded at low elevations aimed at capturing mainly synoptic-scale spatial patterns at low resolution (>100 km). Furthermore, synoptic-scale studies cannot provide reliable insights into the spatiotemporal specifics of climate variability in a mountain belt, since the pronounced orographic and relief gradients strongly impact both total and extreme rainfall patterns.

Moreover, several recent studies have analyzed extreme rainfall events in the Central Andes, (Romatschke and Houze 2010; Boers et al. 2014a, 2015b; Rohrmann et al. 2014; de la Torre et al. 2015; Espinoza et al. 2015). However, none of these investigations have addressed changes in rainfall patterns at the scale of the entire mountain belt, although the Central Andes comprise the catchments for the Amazon and La Plata rivers, including the most populated and economically relevant areas in South America (Tucci and Clarke 1998; Berbery and Barros 2002; Lavado Casimiro et al. 2013; Gloor et al. 2013).

Our study provides a comprehensive analysis of rainfall variability and trends in the subtropical Central Andes of NW Argentina, comparing changes in extreme, total annual and seasonal rainfall along an E-W oriented elevation transect across the Andes. We test if the spatiotemporal rainfall pattern has undergone statistically significant changes during the last six decades (1950–2014), and if so, to which degree magnitude and/or frequency of heavy rain and extreme events account for precipitation variations at annual and seasonal scales. Carefully taking into account both strengths and limitations of the different datasets, we integrate (1) daily, high-quality rain-gauge time series for the period 1950–2014, including stations located both at low and high elevations, and (2) high-spatiotemporal resolution gridded datasets for the period 1979–2014, based on interpolated ground-station observations or remotely-sensed estimations. We define a set of climate indices relevant to both extreme and total rainfall and we analyze their spatiotemporal changes for different time periods starting in 1950. We perform rigorous statistical analyses on rainfall time series, focusing on changes in magnitude and frequency of extreme events using quantile regression (Koenker and Bassett 1978; Cade and Noon 2003), with a particular emphasis on the 95th percentiles.

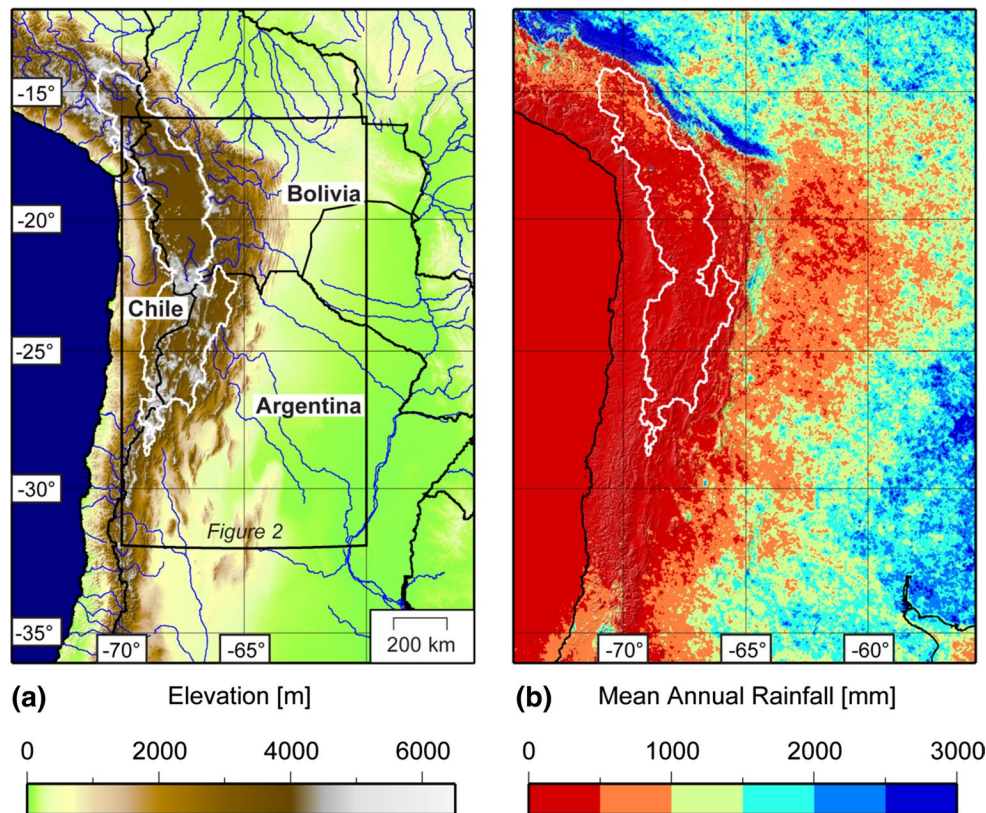## 2 Climatic and geographic setting

The study area lies at the eastern flank of the southern Central Andes between 16° and 32°S (Fig. 1), across the boundary between the tropics and subtropics. This region is characterized by strong contrasts in topography, with lowlands in the east at about 0.5 km asl and high-elevation areas in the west with peaks in excess of 6 km. The western study area is part of the internally drained Andean Plateau, the second largest plateau on Earth, with a mean elevation of about 4 km asl and low topographic relief (Fig. 1). The Andean Plateau can be divided into the northern Andean Plateau (Altiplano), located in the tropics, and the southern Andean Plateau (Puna de Atacama) in the subtropics, roughly below 20°S. In contrast, the area between the eastern low and western high elevations constitutes a region with steep topographic gradient and high relief.

We distinguish between three main topographic areas with distinctive climatic environments that we define as followed from east to west: (1) the *low elevations* (<0.5 km) with low topographic slopes and low relief values; (2) the *intermediate elevations* (also referred to as the mountain front) describes the area with steep slopes and high relief values that abuts the eastern low elevations of the Andean foothills with elevations roughly between 0.5 and 3 km; (3) the *high elevations* above 3 km to the west of the mountain front with steep slopes and high relief. The *intermediate elevations* are characterized by a very dynamic surface-process regime, where steep topographic, environmental, and climatic gradients coincide.

The rainfall pattern in the southern Central Andes is controlled by the interaction between topography and the large-scale atmospheric circulation (Gandu and Geisler 1991; Campetella and Vera 2002; Bookhagen and Strecker 2008; Garreaud et al. 2010; Insel et al. 2010). Moisture transport along and into the southern Central Andes occurs during the wet season, dominated by the South American Monsoon System (SAMS) (Zhou and Lau 1998; Vera et al. 2006; Silva and Carvalho 2007; Marengo et al. 2012). Due to the orographic effect of the Andean orogen, moisture is partly released in form of intense rainfall at the eastern flanks of the tropical Andes and partly advected southward by the South American Low-Level Jet (SALLJ), towards the subtropical areas of South America (Gandu and Silva Dias 1998; Marengo et al. 2012; Boers et al. 2015b). Triggered by the interaction between moisture-laden wind and the orographic barrier, intense precipitation occurs also at the eastern flank of the subtropical southern Central Andes in NW Argentina, resulting in a steep E-W rainfall gradient between the humid low-elevation and semi-arid to arid high-elevation regions (Fig. 1). Here, on average, about 80 % of the total annual rainfall occurs between December and March, when the SAMS is at its mature phase (Rohmeder 1943; Halloy 1982; Bianchi and Yañez 1992; Boers et al. 2015b).

The distribution of rainfall maxima at the windward flanks of the tropical and sub-tropical Central Andes is

Fig. 1 Topographic and climatic characteristics of the southern Central Andes. **a** Topography is derived from SRTM data; boundary of the internally-drained Altiplano (northern Andean Plateau) and Puna de Atacama (southern Andean Plateau) is outlined in *white*. Major rivers are marked in *blue*, *black lines* denote political borders. *Black box* outlines the study area in NW Argentina (cf. Fig. 2), with lowlands at <0.5 km asl in the eastern, the mountain front to the west (0.5–3 km asl) and the high-elevation regions (<3 km asl) further west near the drainage divide of the Andean Plateau, with peaks elevations in excess of 6 km; **b** mean annual rainfall data derived from TRMM 2B31 over the period 1998–2014 (Bookhagen and Strecker 2008; Bookhagen and Burbank 2010). Rainfall is characterized by a pronounced gradient between low-elevation frontal areas and arid, high-elevation areas of the internally drained plateau

controlled by the geometry of the mountain range, its orientation, and small-scale topographic structures, with observed precipitation hotspots that may reach 6 m/year (Seluchi and Marengo 2000; Garreaud et al. 2003; Bookhagen and Strecker 2008; Giovannettone and Barros 2009; Espinoza et al. 2015). Intense rainfall events along the eastern mountain flanks and on the central Andean Plateau both in the tropical and subtropical parts of the mountain range are mainly associated with mesoscale convective systems (MCSs), forming locally and triggered by orographic uplift or atmospheric instability (Maddox et al. 1979; Garreaud 2000; Romatschke and Houze 2013; Boers et al. 2015b). To a lesser degree, MCSs formed in other source areas may propagate to the eastern flanks of the Central Andes (Cohen et al. 1995; Durkee et al. 2009; Boers et al. 2015b). For example, frontal systems originating from the central Argentine lowlands and fed by moisture advected by the SALLJ generate intense rainfall events in the subtropical drainage basins, including the Andean Plateau.

The overall rainfall pattern can be modulated by the interplay of different atmospheric features such as the South Atlantic Convergence Zone (SACZ), the Bolivian High or the Chaco Low (Gandu and Silva Dias 1998; Salio et al. 2002; Carvalho et al. 2004; Vuille and Keimig 2004; Boers et al. 2014c). Also, different climate disturbances such as the Pacific Decadal Oscillation (PDO), the El Niño Southern Oscillation (ENSO), or the Madden-Julian oscillation (MJO) can substantially affect the overall rainfall pattern during the SAMS, by controlling the strength of the SALLJ (Madden and Julian 1971; Vuille et al. 2000; Garreaud and Aceituno 2001; Mantua and Hare 2002). Consequently, anomalously large amounts of moisture can be transported toward subtropical South America, deeply affecting the local rainfall pattern and often resulting in flooding and mass-movement events at the eastern slopes and in the intermontane valleys (Vera et al. 2006; Houston 2006; Boers et al. 2014a).

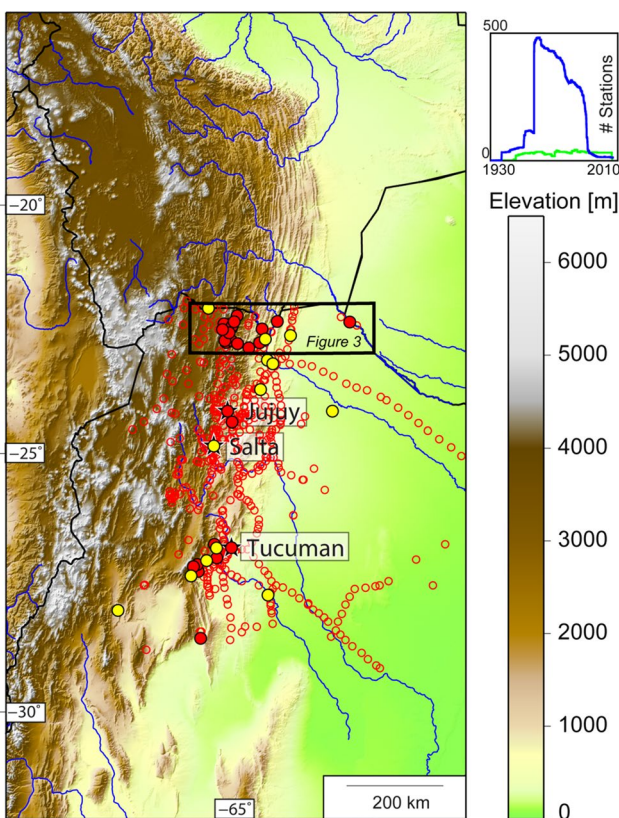Hence, in this region any changes in the rainfall pattern during the summer wet season will also have a strong

impact on water-resource, infrastructure or hydrological risk management. Therefore, in our study we focus our analysis on the summer season (DJF) while the results for the other seasons are available in the Online Resources.
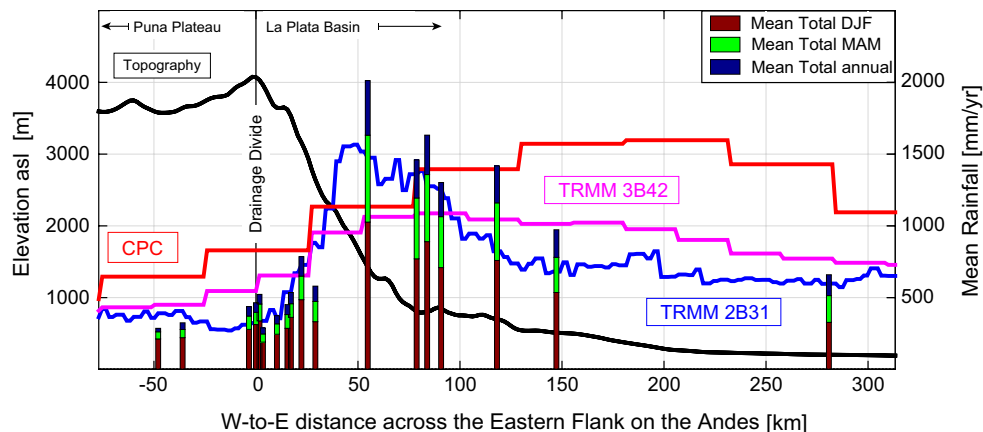
3 Data and methods

We rely on daily-rainfall time series derived from both synoptic meteorological and hydrological stations from the southern Andean Plateau, the eastern flanks of the mountain belt, and the foreland (Fig. 2). To achieve higher spatial and temporal resolution, we included both rain-gauge derived and remotely-sensed gridded datasets retrieved from multiple sources, with different characteristics in spatiotemporal resolution. The data used in this study are:

1. Daily hydrological time series from 1925 to the present, made available in NW Argentina by the Argentine National Weather Forecast Service (Servicio Meteorológico Naciónal, SMN, 592 stations) and by the Department of Water Resources (Subsecretaría de Recursos Hídricos de la Nación, Banco Nacional Hídrico, BNH, 83 stations). Although most of the recording stations are located at the Andean mountain front, several stations also exist in the orogen interior. Unfortunately, during the last two decades a majority of the stations of the SMN network were abandoned due to a reorganization of the monitoring network (Fig. 2). Among a total of 675 rain gauges, a set of 40 high-quality time series was selected in the investigated area. The selection depended on whether the data were continuous with at least 80 % of the expected number of data available over the last three decades (1979–2014) (Haylock et al. 2006; Isotta et al. 2014) and met the standard-quality requirements, assessed using WMO validation standards (WMO 2008; Rodda 2011; Antolini et al. 2015). Time-series homogeneity was tested by visual inspection (Haylock et al. 2006; Longobardi and Villani 2009), since constructing a suitable reference time series was often not possible, given the excessive difference in elevation and/or relative distance between station locations. Among the 40 selected stations, 13 stations operated continuously over the period 1950–2014 (Fig. 2). Table ESM 1 in the Online Resource summarizes the selected station locations and time-series duration in a metadata table.

2. Climate Prediction Center (CPC) unified gauge (CPC-uni): the National Oceanic and Atmospheric Administration (NOAA) CPC unified gauge provides daily rainfall values from 1979 to the present at $0.5° \times 0.5°$ spatial resolution over the global land areas (Xie et al. 2007; Chen et al. 2008). High-quality gauge reports are collected from multiple sources and used to build a daily analysis based on an optimal interpolation technique, which reprojects precipitation synoptic reports to a grid. Several studies on rainfall climatology, testing the performance of climate modeling or comparing different rainfall datasets have used CPC-uni (Higgins et al. 2000; Silva et al. 2007; Jones et al. 2012; Bombardi et al. 2013; Jones and Carvalho 2014; Ruscica et al. 2014; Rao et al. 2015).

3. Tropical Rainfall Measurement Mission (TRMM 3B42 V7): the TRMM Multi-satellite Precipitation Analysis (TMPA) provides 3-h rainfall estimates from January 1998 to September 2014 at $0.25° \times 0.25°$ spatial resolution (Huffman et al. 2007). The gridded rainfall algo-

Fig. 2 Topography of the study area and spatial distribution of 675 meteorological stations measuring daily rainfall (592 from SMN and 83 from BNH) in the provinces of Jujuy, Salta, Tucumán, Catamarca, and Santiago del Estero in NW Argentina (for location see Fig. 1). *Unfilled red circles* indicate the location of rainfall stations that have been in operation during the period 1925–2014; *Filled red circles* represent the location of 40 rainfall stations that have been operating continuously between 1979 and 2014, among which 13 have continuous rainfall time series back to 1950 (*yellow filled circles*). Graph in *right upper corner* depicts temporal evolution of the number of active stations operating in the target area during the last 90 years (*blue* SMN; *green* BNH). Significantly less station data were collected in the last two decades. The *black rectangle* denotes the area of the swath profile in Fig. 3

Fig. 3 Swath profile (100 km wide, 390 km long) showing longitudinal variability of rainfall and topography (cf. Fig. 2 for swath location). Rainfall data show annual average amounts from both station data (CLINO 1981–2010) and gridded datasets (CPC, *red*, 1979–2014; TRMM 3B42, *magenta*; and TRMM 2B31, *blue*, 1998–2014). Note strong E–W rainfall gradient, best depicted by rain-gauge and high-spatial resolution TRMM 2B31 data: mean annual rainfall increases up to 2000 mm/year when the first orographic barriers are reached at ~50 km distance from the drainage divide. Rainfall rapidly decreases to <500 mm/year in the lee of the orographic barriers. Seasonal contributions to annual mean totals for austral summer (DJF) and autumn (MAM) show that these two seasons alone account for at least 70 % of the annual totals. Quantitative and qualitative comparison reveals that TRMM 2B31 estimations are in good agreement with station-derived values (Bookhagen and Strecker 2008, and this study), whereas the lower spatial resolution TRMM 3B42 data is less capable to correctly detect the location of rainfall maxima at the orographic barrier

rithm uses an optimal combination of TRMM 2B31 and TRMM 2A12 data products, SSM/I, Advanced Microwave Scanning Radiometer (AMSR), and Advanced Microwave Sounding Units (AMSI) (Kummerow et al. 1998, 2000). Here we used the research-grade version, which is calibrated at monthly scale using land-surface precipitation-gauge analysis based on the GCPC dataset (Huffman et al. 2007). Previous studies used TRMM 3B42 data to analyze rainfall variability providing high-quality estimates in South America and other regions (Carvalho et al. 2012; Chen et al. 2013; Xue et al. 2013; Boers et al. 2015a) to identify rainfall-extreme events and their impact on river discharge, to develop a method for predicting extreme floods in the eastern Central Andes. Furthermore, these data were used to spatially characterize and identify the origin of rainfall over South America (Bookhagen and Strecker 2011; Boers et al. 2013, 2014a, b, 2015a, b). TRMM 2B31 data with 5 km x 5 km spatial and approximately daily resolution were also used to relate topographic characteristics and orographic rainfall along the eastern Andes (Bookhagen and Strecker 2008).

A ~100-km-wide and 390-km-long longitudinal swath profile (22°–23°S, 66°–62°W) shows the pronounced topographic and rainfall gradients across the Andes, detected by station data and CPC-uni and TRMM products (Fig. 3). Previous studies showed that the TRMM 3B42 V7 and CPC-uni data provide a statistically robust description of

the main features of the SAMS (Carvalho et al. 2012; Boers et al. 2015b). However, there are significant uncertainties in the characterization of extreme precipitation events using the coarser gridded climatic datasets (Ensor and Robeson 2008; Carvalho et al. 2012).

Based on the collected data, we estimated annual and seasonal values (SON, DJF, MAM, JJA) of several indices (Table 1), for the rainfall-data parent distribution and for the extreme values, both at yearly and multi-decadal scales [mean values for climatological normals (CLINO, World Meteorological Organization 2011) 1961–1990 and 1981–2010] for different time periods (1950–, 1979–, 1998–2014), for which the selected datasets were available. For the daily datasets, we define *wet days* as all occurrences larger than 0.5 mm/day and for the 3-h dataset *wet hours* as those occurrences exceeding 0.1 mm/3 h. Our statistical analysis was performed using years/seasons with less than 20 % missing data. We focused our analysis on the temporal evolution of these indices evaluating yearly deviations from the CLINOs as absolute anomalies. Given the index X, the yearly (annual/seasonal) absolute anomaly is defined as $AX_i = X_i - <X>$, where X_i are the annual/seasonal estimation for X in the i-th year (i = 1, …, N, N = length of the time series in year), and $<X>$ the relevant CLINO estimation. We also analyzed normalized values of the climate indices by the mean CLINO values to achieve an unambiguous interpretation of differences in the rainfall pattern between wet and dry areas. In the following, we will refer to *mean-normalized* anomaly as defined by: $ANX_i = 100*AX_i/<X>$ and expressed in %/year.

Table 1 List of climate indices evaluated for analyzing climate spatiotemporal variability in NW Argentina

Abbreviation	Parameter	Units
TS	Total amount	mm/year
TSF (TSF %)	Absolute (percentage[a]) fraction due to the seasonal totals to the annual amount	mm/year (%/year)
#WD	Number of wet days (>0.5 mm/day)/hours (>0.1 mm/3 h)	#/year
MRd	Mean daily/3-h rainfall for wet days/hours	mm/day mm/3 h
IthPrct	Ith percentiles of wet days (I = 1, 5, 10, 25, 50, 75, 90, 95, 99, 99.5 99.9)	mm
#IthPrct (%IthPrct)	Number (percentage with respect to the total number of wet days/hours) of wet days/hours exceeding the Ith percentile	#/year (%/year)
TPIthPrct (TP %IthPrct)	Absolute (percentage[a]) fraction of TS accounted for by wet days/hours exceeding the Ith percentile	mm/year (%/year)

All indices were estimated at annual as well as seasonal (SON, DJF, MAM, JJA) scale

[a] The percentage is estimated dividing the absolute value by the relevant total amount (year/season)

Despite recent advances in the calculation of the distribution of rainfall extremes (e.g., AghaKouchak and Nasrollahi 2010; Papalexiou and Koutsoyiannis 2013; Serinaldi and Kilsby 2014), drawbacks regarding the evaluation of power-law exponents for these distributions still exist, especially related to model regressions based on low-populated samples. In our study, instead of evaluating distribution fitting parameters, we applied quantile regression analysis (Koenker and Bassett 1978; Cade and Noon 2003) to the wet days subsets of the raw data, to detect if rainfall-frequency distributions underwent statistically significant changes in the mean/median values as well as in the higher extremes during the past decades. In the appendix a short description of the quantile regression methodology is provided.

We estimated several percentiles (Table 1) focusing on extreme wet days and defined in the statistical sense *low-moderate* and *extreme* rainfall events as those occurrences below the 50th and exceeding the 95th percentiles, respectively (Wulf et al. 2012; Boers et al. 2014a; Espinoza et al. 2015).

For deciphering and interpreting the evolution of both rainfall-frequency and intensity for semi-arid to arid environments, we estimated climate indices, including percentiles, restricting the analysis to the wet days/hours subsets, adopting the standard practice commonly applied to climate studies (e.g., Tank et al. 2009; Rajczak et al. 2013; Sillmann et al. 2013; Kendon et al. 2014). Additional information can be found in the Online Resource.

We analyzed the evolution of the percentiles of the wet days/hours frequency distributions using normalized wet days/hours subsets of data, to allow for a spatial comparison in a region characterized by pronounced spatial variability. We will refer to it below as *median-normalized*, having divided each original wet days/hours sub-datasets by the 1981–2010 median of the frequency distribution of the wet days/hours. For the TRMM dataset (1998–2014)

no CLINO values could be estimated and the normalization was obtained using the 1998–2014 median values. We emphasize that only in the case of the percentile indices the median-normalization was performed.
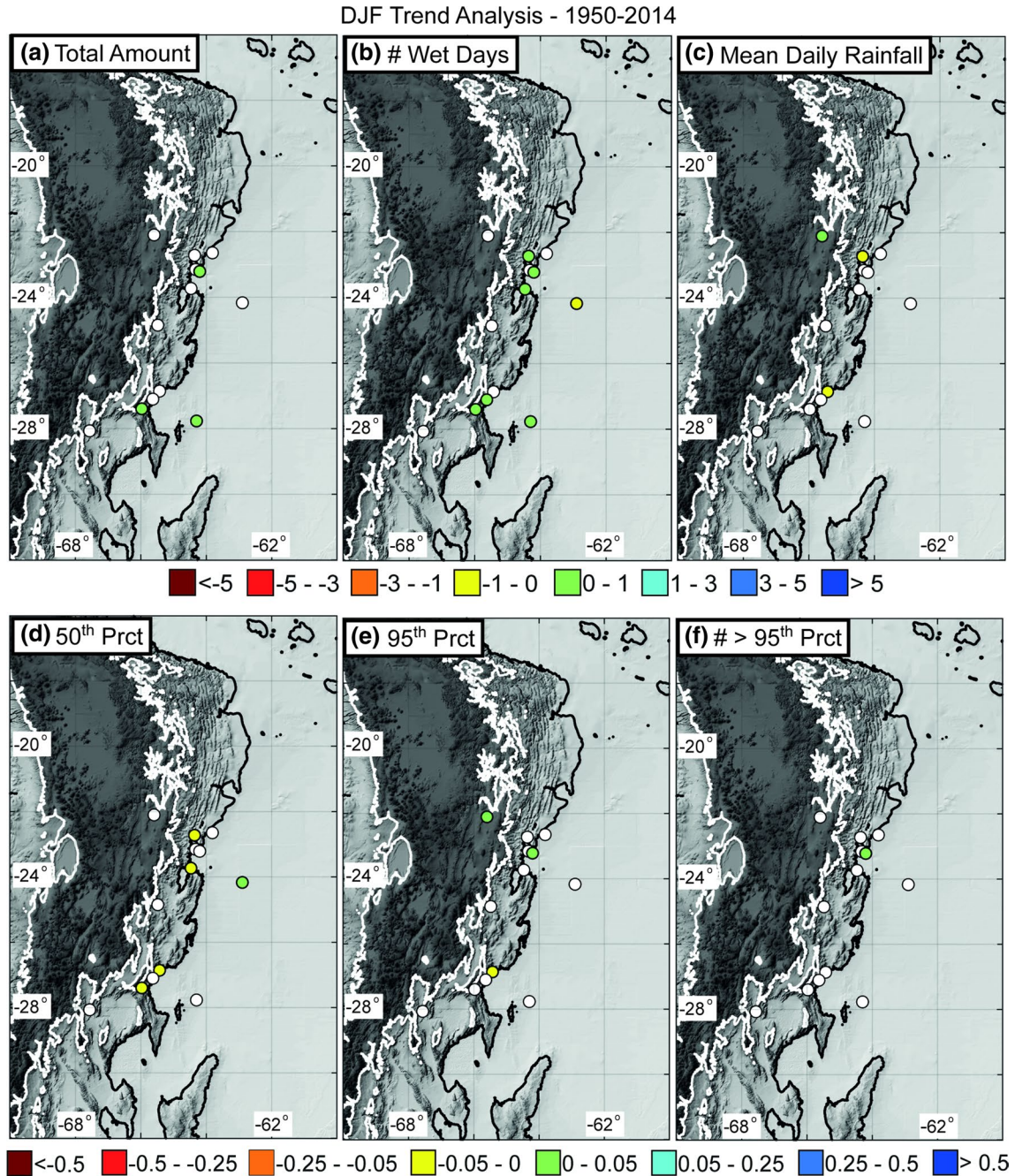
Except for percentiles, trends associated with every climate index were estimated applying iteratively re-weighted least squares with a bisquare-weighting function (Holland and Welsch 1977; Huber 1981). In the following we will refer to the latter analysis as *robust regression*. For all indices, including percentiles, trends are represented by the slope of the regression line and the statistical significance was verified applying a two-tailed t-Student test at the 95 % confidence level (Gosset 1908; Yue and Pilon 2004).

4 Results

4.1 Trend analysis for the period 1950–2014

Rainfall time series are available for this time period only from rain gauges. Although some time series start in the 1920s, we performed our statistical analysis starting in 1950, for which a sufficiently populated statistical ensemble can be configured with 13 stations located in the humid and arid regions. All analyses were conducted on annual and seasonal time scales; in the data presentation DJF trends are shown for all 13 rain gauges, revealing a complex spatiotemporal pattern (additional data plots are in the Online Resources, Figs. ESM 2–6).

Our study confirms that the steep orographic rainfall barrier in the southern Central Andes results in a pronounced rainfall gradient across the Andean orogen (Fig. 3) (Bookhagen and Strecker 2008; Rohrmann et al. 2014). The mean rainfall pattern in NW Argentina is associated with strong seasonality, with summer and fall seasonal totals (6 months) on average accounting for at least 70 % of the annual values (Fig. 3) (e.g., Vera et al. 2006;

Fig. 4 Trend analysis of daily rainfall estimation from rain gauges for DJF for the period 1950–2014 (for this period 13 stations were available). *Black* and *white lines* are elevation contours at 500 and 3000 m asl, respectively, roughly separating the eastern lowlands from the intermediate and high-elevation areas to the west. Shown are the mean-normalized climate indices **a** total amount, **b** number of wet days, **c** mean daily rainfall ([% year^{-1}]); the median-normalized climate indices **d** 50th percentile, **e** 95th percentile ([year^{-1}]), and **f** the mean-normalized number of events exceeding the 95th percentiles ([% year^{-1}]). *Full circles* are statistically significant trends at $p < 0.05$ confidence level, *empty circles* are non-significant values; approximately half of the stations presents statistically significant results (see also Fig. ESM 6A)

Bookhagen and Strecker 2008; Espinoza et al. 2015; Boers et al. 2015b).

Approximately half of the analyzed stations provided statistically significant ($p < 0.05$) trends for DJF (Fig. 4).

The data show a rather coherent spatial pattern for DJF total amount and number of wet days indices, with most of the significant trend signal observed at the transition zone between low and intermediate elevations (0.3–1.5 km)

(Fig. 4 and Fig. ESM 5). Total amount and number of wet days indices increased during the period 1950–2014 at the transition zone between the low and intermediate elevations, whereas low elevations exhibited a more mixed pattern (Fig. 4a, b). Mean daily rainfall showed positive trends at high elevations, but there were negative trends at the mountain front (Fig. 4c). Quantile regression indicated negative trend values for the 50th percentile at the transition zone between the low and intermediate elevations and positive values at low elevations (Fig. 4d). Fewer stations provided significant trends for the 95th percentile, with positive trends at the northernmost stations at high elevations and at the transition zone between the low and intermediate elevations, whereas almost no trend is found for the frequency of events exceeding the 95th percentile (extreme events). In the following, we denote the area where the northernmost stations are located as *the northernmost NW Argentine provinces*. Though based on few stations, both magnitude and frequency of the 95th percentile presents non-significant trends at low elevations, whereas a positive trend is found at high elevations (Fig. 4e, f).

4.2 Trend analysis for the period 1979–2014

Both rain-gauge time series (40 stations) and the CPC-uni dataset (hereafter referred to CPC) are available for this time period. Station data showed mostly no significant trends for the total amount for DJF. On the contrary, the frequency of wet days exhibited negative trend values at low elevations, a more mixed pattern at the mountain front, and mostly no significant values at high elevations (Fig. 5a, b). CPC indicated similar trend patterns of the number of wet days at low elevations, with mostly significant negative trends as low as −3 %/year in the lowlands. CPC also exhibited large areas at high elevations (between 20° and 17°S and between 30° and 25°S) with significant positive trends of up to 5 %/year or more particularly for the total amount. For mean daily rainfall, few stations provide significant results, exhibiting a mixed pattern of significant trends at the mountain front for the southernmost stations and negative trends at high elevations for the northernmost ones. CPC for this index showed positive trends both at low and high elevations, with more pronounced and coherent trends in the high-elevation regions up to 5 %/year (Fig. 5c). Quantile regression for rain gauges documented relatively low trend values for the 50th percentile; the 95th percentile exhibits a more mixed pattern with no significant trend at low elevations, mainly negative at high elevations, and positive in the transition between the low and intermediate elevations, where also the frequency of extreme events showed positive trends (Fig. 5d–f). For CPC, we observed that for DJF the 95th percentile trend pattern exhibits
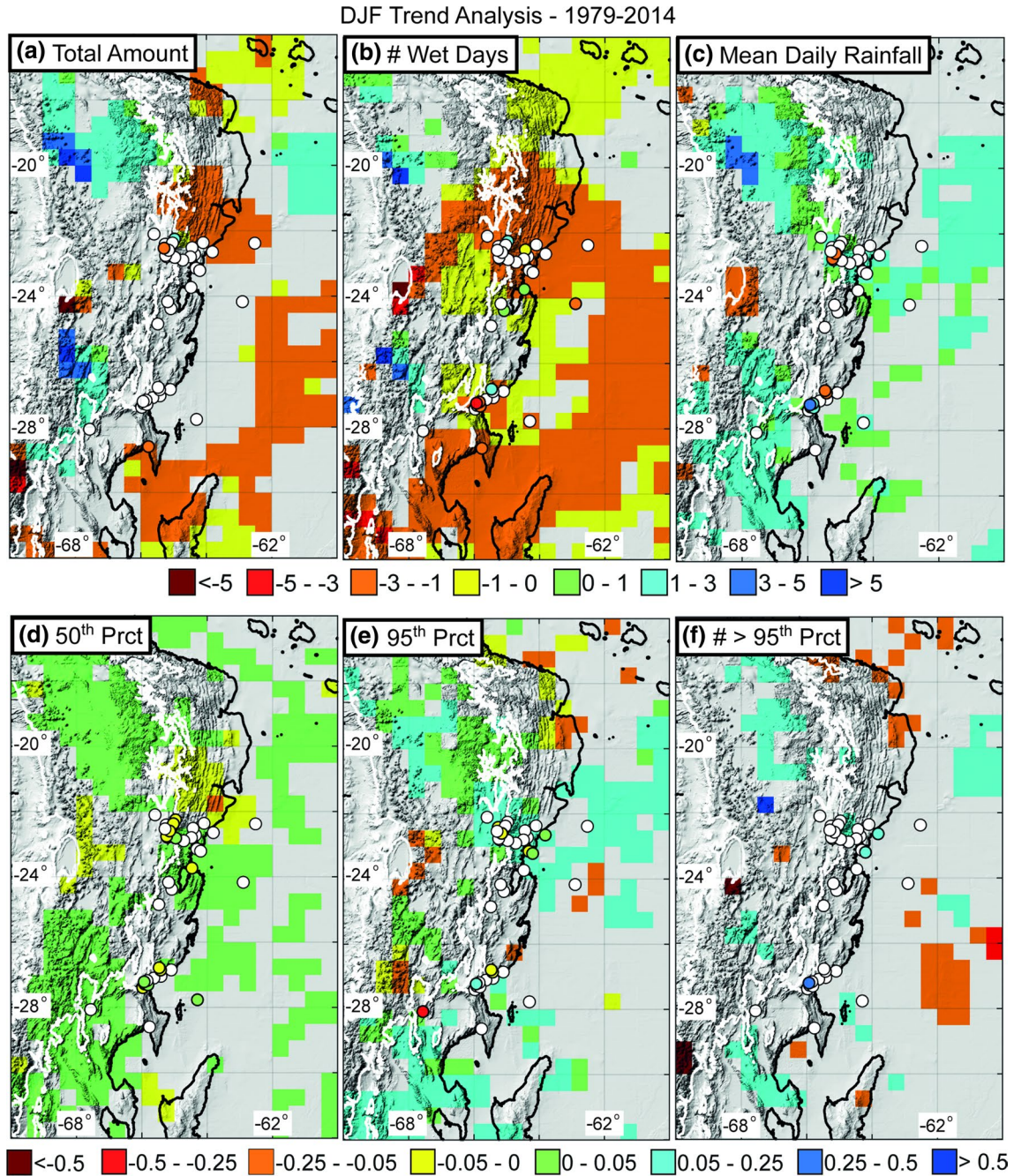
extensive regions characterized by positive trends both at low and high elevations (up to more than 0.25–0.5 times the value of the median in a year), associated with a less coherent and more mixed trend pattern of the frequency of extreme events (≥95th Prct) for DJF (Fig. 5f). On the contrary, the 50th percentile exhibited trend values of low significance (Fig. 5d). Acceptable agreement is found between rain gauges and CPC results at low elevations and at the mountain front, but there are significant differences at high elevations (Fig. 5b, c, f).

4.3 Trend analysis for the period 1998–2014

TRMM 3B42 V7 data (hereafter referred to TRMM) were used to analyze rainfall-trend patterns for the period 1998–2014. TRMM were aggregated at daily scale (12UTC–12UTC) to obtain the same time resolution of the stations and CPC data sets, and the same methodology was applied to both 3-h (raw-data time resolution) and daily rainfall datasets. Daily and 3-h datasets exhibited analogous spatiotemporal patterns (Fig. ESM 6C). In the following, results obtained for the 3-h dataset will be shown. As in the previous cases, trend analyses were conducted at annual and seasonal scale (Table 1) and results for the summer (DJF) are shown (see Online Resources for complete results).
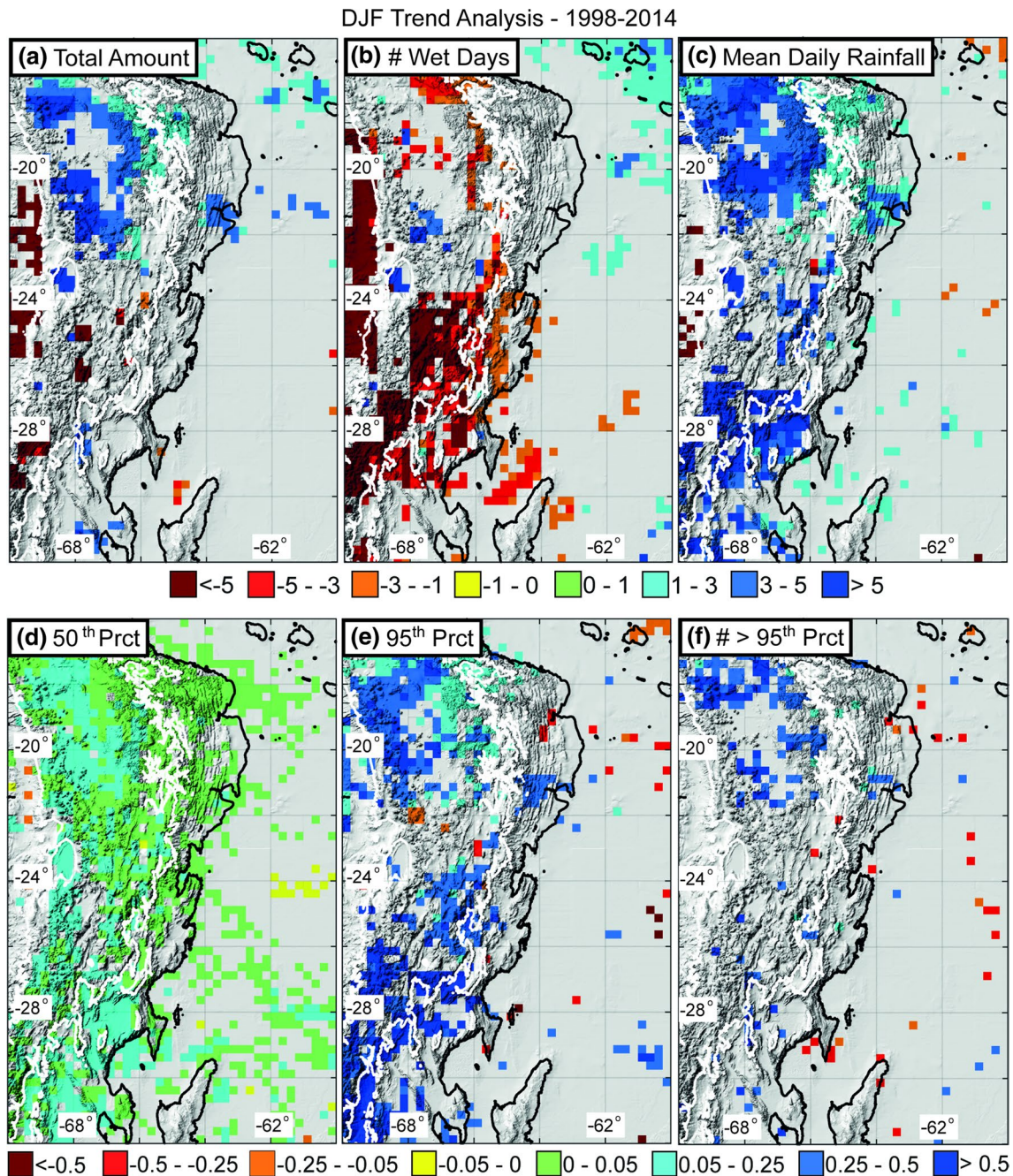
Total amount, number of wet hours, and mean 3-h rainfall climate indices display different patterns, especially at high elevations (Fig. 6a–c): the total amount shows significant trends mainly in the northernmost part of the study area (23°–17°S) and mostly positive (with values exceeding 5 %/year), whereas the number of wet hours exhibits significant trends mainly concentrated in the southernmost area (below 23°S), and generally negative (with values <−5 %/year). As a consequence, the mean 3-h rainfall shows mainly positive trends, especially at high elevations up to more than 5 %/year. In the low-elevation regions few grid cells exhibited statistically significant trends for these indices. In particular, total amount and number of wet hours showed positive trends in the northernmost part of the study area (above 23°S), whereas the southernmost region (below 25°S) is characterized by mostly negative trends.

For the wet hours frequency distribution, we observed that during DJF the 50th percentile exhibits mostly no or relatively low significant trends (Fig. 6d); in contrast the 95th percentile records a coherent trend pattern with large regions characterized by positive trends, especially in the high-elevation regions (up to more than 0.5 times the value of the relevant percentile in a year, Fig. 6e). We observed that the overall pattern of the 95th percentile generally mimics mean daily rainfall (Fig. 6c). During DJF the frequency of extreme rainfall events (≥95th Prct) exhibits few significant, but mainly positive trends at high elevations.

Fig. 5 Trend analysis of daily rainfall estimation from rain gauges for DJF for the period 1979–2014 (for this period 40 stations are available) and CPC dataset. *Black* and *white lines* are elevation contours at 500 and 3000 m asl, respectively, roughly separating the eastern lowlands from the intermediate and high-elevation areas to the west. Shown are the mean-normalized climate indices **a** total amount, **b** number of wet days, **c** mean daily rainfall ([% year^{-1}]); the median-normalized climate indices **d** 50th percentile, **e** 95th percentile ([year^{-1}]), and **f** the mean-normalized number of events exceeding the 95th percentiles ([% year^{-1}]). Rain gauges: *Full circles* are statistically significant trends at $p < 0.05$ confidence level, *empty circles* are non-significant values; few stations provided statistically significant results (approximately ¼ of the stations). CPC dataset: only statistically significant trends are shown ($p < 0.05$; blank grid cell are non-significant trends; between 17 and 58 % grid cells provide significant results (Fig. ESM 6B)

Fig. 6 Trend analysis of 3-h rainfall estimation from TRMM 3B42 dataset for DJF over the period 1998–2014. *Black* and *white lines* are elevation contours at 500 and 3000 m asl, respectively, roughly separating the eastern lowlands from the intermediate and high-elevation areas to the west. Shown are the mean-normalized climate indices **a** total amount, **b** number of wet days, **c** mean daily rainfall ([% year^{-1}]); the median-normalized climate indices **d** 50th percentile, **e** 95th percentile ([year^{-1}]), and **f** the mean-normalized number of events exceeding the 95th percentiles ([% year^{-1}]). Only statistically significant trends are shown ($p < 0.05$; blank grid cell are non-significant trends); between 17 and 28 % grid cells provide significant results

5 Discussion

5.1 Caveat

Gridded-rainfall data are a useful source of information for several types of studies, particularly for an assessment of climate variability and climate-change analyses (Dai et al. 1997; Sen and Habib 2000; Sen Roy and Balling 2004; Carvalho et al. 2012; Boers et al. 2014a, 2015b), because they avoid the limitations of point observations with uneven spatial distribution or missing data (Daly et al. 1994; Liebmann and Allured 2005; Daly 2006; Ensor and Robeson

2008). However, it has been long recognized that ground-station based gridded rainfall data have limitations as well, especially at high temporal resolution. In particular, the spatial density of the original rain gauges is reflected in the quality of the interpolated values (Ensor and Robeson 2008; Carvalho et al. 2012). For the CPC dataset it has been observed that, besides good agreement between annual and seasonal total amounts (TS), the frequency of low-magnitude events is overestimated, whereas both frequency and magnitude of heavy-rain events are usually underestimated (Ensor and Robeson 2008). This behavior will affect the wet days frequency distribution, will shift the percentiles towards lower values, and may also impact the total amount at annual and seasonal scales. We argue that by shifting the frequency distribution towards low values, lower variability will characterize the rainfall gridded dataset, implying potentially lower trends than provided by the original rain-gauge time series. Although it is not the aim of this study to test the degree of agreement between the rain gauges and the CPC datasets, we still need to take into account these limitations for correctly interpreting the outcomes of the statistical analysis.

We also point out that, as a consequence of the limited number of measuring stations in remote mountainous areas such as in our study area, the gridded and interpolated rainfall patterns may be misrepresented, especially at high elevations, including the Puna de Atacama Plateau and mountain-front areas, characterized by steep climatic and topographic gradients (Bookhagen and Strecker 2008, 2012). Figure 3 illustrates this constraint with a longitudinal swath profile, highlighting the rainfall gradient across the NW Argentine Andes. Visual inspection reveals that the high-spatial resolution TRMM 2B31 estimations are in good agreement with station-derived values (Bookhagen and Strecker 2008). With decreasing spatial resolution, however, we are less capable to correctly detect the location of rainfall maxima at the orographic barrier. In particular, the CPC dataset is less precise in localizing the rainfall maxima at the mountain front, and it overestimates rainfall amounts in the arid, high-elevation region. Here, rainfall peaks in the lee of the eastern ranges record values twice as high as station estimates. We argue that trend-analysis results based on the CPC dataset may be affected by lower absolute trends and that spatial location of maximum and minimum estimations may be misrepresented, particularly within topographic transitions, compared to the rain-gauge dataset.

Furthermore, although based on calibrated remotely-sensed measurements, research-grade TRMM estimations can be potentially affected by bias errors in remote high-elevation regions as well. In fact, among other sources of uncertainty affecting TRMM evaluations, the calibration strongly depends upon the density of the ground stations (Huffman et al. 2007), which is limited in high-elevation areas. Several studies have addressed this issue (e.g., Condom et al. 2011; Heidinger et al. 2012; Zulkafli et al. 2014; Nerini et al. 2015; Wulf et al. 2016). Most of these studies analyzed the performance of satellite observations for hydrological applications at drainage-basin scale, which requires continuous and high-quality rainfall estimates. It has been shown that TRMM data overestimate rainfall compared to rain-gauge measurements in areas of pronounced relief. Thus, post-processing and rainfall adjustment in combination with ground observations are an approach to rescale these data for hydrological applications (e.g., Wulf et al. 2016). At the same time, the comparison of the performance of TRMM with other rainfall-gridded datasets reveals that TRMM sufficiently captures the major features of SAMS with respect to the other datasets (Carvalho et al. 2012; Boers et al. 2015a). Also, Boers et al. (2015b) have shown that TRMM allows detecting the propagation of extreme events from the southeastern sectors of South America towards the eastern Central Andes, whereas reanalysis datasets at coarser resolution, such as ERA-Interim (Dee et al. 2011) and MERRA (Rienecker et al. 2011), could not reproduce this mechanism. Thus, depending on the specific application, particular caution must be used to correctly interpret results based on TRMM data. We emphasize that in the present study, we relied on normalized indices to analyze changes in the rainfall field, which should filter out systematic overestimations.

Station data from high-elevation environments have inherent limitations as well, mainly related to uneven spatial distribution of rain gauges, a problem often dictated by maintenance and infrastructure conditions in these regions. Despite the fact that rain gauges provide high-quality observation, in some cases the rainfall stations used in our study are located at valley bottoms, particularly in the transition between low and high-elevation areas. These stations may not represent an area average, but are only representative of the climatic conditions for a restricted area.

In our analyses, we carefully took into account the strengths and limitations of the various datasets. With these boundary conditions in mind, we aimed at testing whether trends in rainfall patterns in the NW Argentine Andes were detectable and to what degree the collected datasets were able to exhibit this signal.

5.2 Rainfall trend at seasonal scale during the period 1950–2014

We observed that total rainfall amount and number of rainy days generally exhibit a positive trend during DJF at the transition zone between the low and intermediate elevations. Importantly, this trend was also found for MAM (Fig. ESM 6), implying that in this area the wet season tends to

get wetter, with both increasing total amount and frequency of rainfall events. On the other hand, we observed either no change or a decrease of total amount and event frequency during SON and JJA (Fig. ESM 6), suggesting that the dry season tends to get drier, which is also evident when plotting the seasonal trends versus elevation (Online Resources, Fig. ESM 5). This behaviour has been defined as 'the wet get wetter, the dry get drier' mechanism (Held and Soden 2006; Carvalho and Jones 2016). However, at the transition zone between the low and intermediate elevations the net annual budget exhibits the trend towards a wetter general condition (Figs. ESM 5–6), in good agreement with results obtained for South America from previous studies (Barros et al. 2000; Haylock et al. 2006). Barros et al. (2000) found positive DJF total amount trends for most of the Argentine territory, more pronounced in the northern study area and during the period 1956–1991, which they related to a decrease of the mean meridional gradient of temperature affecting atmospheric circulation. Their results were also confirmed by Haylock et al. (2006) with a comprehensive study of rainfall trends in South America during the period 1960–2000, suggesting wetter conditions at annual scale for northern Argentina.

5.3 Rainfall trend at seasonal scale during the period 1979–2014

We have performed a trend analysis for a shorter period (1979–2014), for which we could rely on a denser rain-gauge network (40 stations) and on the CPC dataset. In contrast, for the period 1950–2014, station data show no trends or a decrease of total amount and number of wet days both at high and low elevations at annual and seasonal scales for 1979–2014 (Fig. 5 and Figs. ESM 5). However, the wet season (DJF and MAM) also exhibits a trend of increasing rainfall (both total amount and number of wet days) at a few localities at the mountain front (Fig. 5). These findings are partially corroborated by the CPC trend analysis, which displays the general trend towards drier conditions for the same period (1979–2014) during DJF, except at high elevations (Fig. 5), where we observed extensive areas of increasing rainfall totals (between 17°S and 20° and between 25°S and 30° and), in part on the Puna de Atacama Plateau. Although for a shorter time period (1998–2014), the TRMM dataset exhibits similar features at high elevations during DJF (Fig. 6), with an area of increasing rainfall on the Puna de Atacama Plateau (between 23° and 20°S). Unfortunately, no station data are available for these areas at high elevation exhibiting significant trends. However, since TRMM data show a coherent trend signal over a wide region, we suggest that this signal represents a real trend towards increasing rainfall at high elevations. Nevertheless, we observed that the local maxima trend values shown by

TRMM at high elevations appear to be displaced southward compared to the CPC outcomes. Such dislocation in the position of maxima and minima trend values is not surprising, since it was recognized that the CPC dataset is affected by such limitations due to the scarcity of rain gauges in the transition between the low and high elevations and the Puna de Atacama Plateau (see Caveat section). Concerning the remaining seasons, both station data and CPC datasets document a trend pattern for Autumn (MAM), which mimics the summer trend, whereas for the dry season (JJA and, to a lesser degree, SON) the tendency towards drier conditions was even more pronounced compared to the period 1950–2014 (Figs. ESM 5–6).

In summary, for the last three decades (1979–2014) we observed a general trend towards drier conditions at low elevations during the wet season and locally wetter conditions at the mountain front. On the contrary, we found evidence for extensive areas exhibiting a trend of increasing total seasonal rainfall amount in the arid Puna de Atacama Plateau region.

Interestingly, the aforementioned positive trend revealed in our study appears to be in contrast with rainfall projections for a different emission scenario for the northern Andean Plateau (Altiplano) obtained during recent studies (Urrutia and Vuille 2009; Minvielle and Garreaud 2011; Thibeault et al. 2012). In particular, Urrutia and Vuille's (2009) projections for DJF rainfall in the tropical Andes during the period 2071–2100 exhibits a rather incoherent pattern, with increasing, as well as decreasing total rainfall amounts compared to the period 1961–1990. On the Bolivian Altiplano the projection showed a significant total-amount decrease. We emphasize that our study area was only partially included in their investigated region. Urrutia and Vuille (2009) suggest that the rainfall decrease expected for DJF by the end of the century could be linked to the weakening of the easterlies in the middle and upper troposphere. It has been recognized that easterly wind anomalies at high tropospheric levels are associated with deep convection on the Altiplano by transporting moist air from the interior of the continent. This phenomenon has been called the 'easterly/wet–westerly/dry relationship' (Garreaud and Aceituno 2001; Thibeault et al. 2010). Minvielle and Garreaud (2011) analyzed the predicted change in rainfall pattern in the Central Andes (15°–25°S) for the end of the twenty-first century (2070–99), confirming a significant decrease in total amounts linked to the change in the middle and upper troposphere circulation with respect to 1970–99. Unfortunately, their study does not include statistically significant results for NW Argentina. Thibeault's et al. (2012) projections also suggested a decrease of rainfall on the Bolivian Altiplano, starting already in 2020, although the implications for the precipitation on the southern Andean Plateau were not discussed.

Fig. 7 Trend analyses for rain gauges (only statistically significant trends, $p < 0.05$, are shown): **a** mean daily rainfall (MRd) trends versus percentile (Prct) trends for the period 1950–2014. The rainfall spatial variability exhibits a complex pattern, reflected both in the mean daily rainfall and in the percentile analysis, with either positive (intensification) or negative (attenuation) trends. All analyzed stations show the same trend for their mean daily rainfall and the frequency distribution percentiles, implying that an intensification of the mean daily rainfall is accompanied by either no change or an intensification of the uppermost percentiles. **b** Same as (**a**) but for the period 1979–2014, indicating similar features. In both periods, attenuation is mostly associated with the dry season, whereas the wet season reflects both attenuation and intensification of rainfall events

To summarize, several studies have suggested a general decrease of rainfall-total amount starting by 2020 for the wet season in the tropical Central Andes. The authors are not aware of similar studies extending their investigation areas southward, including the Puna the Atacama plateau (southern Andean Plateau) in NW Argentina, which has different climatic characteristics than the Bolivian Altiplano (northern Andean Plateau), in particular concerning the characteristics of rainfall convective systems (Romatschke et al. 2010; Romatschke and Houze 2013; Rohrmann et al. 2014). However, the CMPI5 projections for rainfall in South America for the end of this century proposed by Carvalho and Cavalcanti (2016) exhibit a more complex pattern for the areas including the northern and southern Andean plateaus. These projections show an overall weak signal of change for the entire wet season (October–March), a negative signal in the Chilean part, and locally a positive signal on the Argentine side. Additionally, Carvalho and Cavalcanti (2016) suggested an intensification of the SAMS poleward of 20°, accompanied by a reduction of up to 40 % of DJF rainfall in Chile. This confirms the different dynamic climatology of the northern Altiplano, located in the tropics, and the subtropical Puna de Atacama Plateau, although both areas are characterized by similar elevations and orography.

Finally, we observe that for the period 1950–2014 there is no clear pattern at low elevations, in contrast with the coherent negative trend for the period 1979–2014. We tested the hypothesis if this change in the trend pattern is related to the 1970s climate shift (Minetti and Vargas 1998; Rusticucci and Penalba 2000; Carvalho et al. 2011; Jacques-Coper and Garreaud 2015); detailed information on this test is provided in the Online Resource. However, based on our station dataset it is not possible to unambiguously identify the 1970s climate shift as a forcing factor of the changing rainfall trend in our study region.

5.4 Trend of daily rainfall magnitude-frequency distribution

As previously pointed out, daily station data showed that DJF mean daily rainfall for the period 1950–2014 recorded few significant values; they are negative at the transition between the low and intermediate elevations, and positive at high elevations (Fig. 4). In contrast, a rather incoherent spatial pattern was observed for 1979–2014 (few significant values, both negative and positive, Fig. 5). On the other hand, both CPC and TRMM results exhibit a coherent signal toward an intensification of the mean-rainfall amount per event, which was particularly pronounced at high elevations (Figs. 5 and 6). This intensification is associated with a diffuse reduction in the frequency of rainfall events, except for restricted areas at high elevations (see Sect. 5.3). Thus, to decipher whether such changes in the mean-rainfall amount per event are due to changes in mean/median and/or to the extreme rainfall values, we analyzed the trends of the different percentiles of the frequency distributions.

The spatial pattern of the percentile trends is in good agreement with the trend shown by the mean daily rainfall-climate index (for station data: Fig. 7, for CPC data: Fig. 5; for TRMM data: Fig. 6). An intensification (or attenuation) of the mean daily rainfall is accompanied by an intensification (or an attenuation) of the percentiles at any order, particularly at high orders (≥90th Prct) (Fig. 7). We also observed that often small or no changes in the median values of the wet days frequency distributions were associated with significant trends, either towards local intensification or attenuation in the 95th percentiles (Fig. 7 and Fig. ESM 3).

In the high elevations of the Puna de Atacama Plateau in the northernmost NW Argentine provinces, DJF extreme events (≥95th Prct) increased in magnitude, but not in frequency during the period between 1950 and 2014, whereas the low-medium events (<50th Prct) exhibit no changes (Fig. 4 and Fig. ESM 11). This results in increased mean daily rainfall without strongly affecting the total amount and frequency of wet days. At the mountain front, few stations provided significant results and the overall trend signal is mixed and not significant. Nevertheless, we observe that, despite a decrease of low-medium events intensity, at few locations in the northernmost NW Argentine provinces both frequency and magnitude of extreme events increased, which is reflected by the total amount and frequency of rainy days. In the southernmost stations, both low-moderate and extreme events exhibit a decreased magnitude, but it is the increased frequency of low-moderate events (Fig. ESM 11) that accounted for the increased total amount and frequency of wet days. At low elevations, non-significant patterns were detected. Taken together, these observations suggest that in the northernmost NW Argentine provinces for the period 1950–2014, extreme (≥95th Prct) events increased in magnitude at high elevations on the Puna de Atacama Plateau and locally at the transition zone between the low and intermediate elevations.

Except for minor discrepancies, the gridded datasets from the periods 1979–2014 and 1998–2014 record increasing magnitude and frequency of extreme events at the mountain front; these trends, do not affect the total amount and number of wet days. Good agreement exists also at low elevations, where the decrease of total amount and number of wet days is not related to changes in extreme events. At high elevations few station data show significant, decreasing magnitudes of extreme events. This result contrasts with findings obtained from CPC and TRMM data, documenting a coherent pattern of increasing magnitude of extreme events for extensive areas on the Puna de Atacama Plateau (between 22° and 20°S and below 24°S). Given that station data provide few significant results for the high elevations among mostly non-significant trends, we

suggest that in this context stations represent only locally the changing character of precipitation, whereas the gridded dataset provides a regional-scale signal of changes of the rainfall pattern.

In summary, our results suggest that at the transition zone between the low and intermediate elevations and in the semi-arid/arid high-elevation areas of the southern Central Andes extreme rainfall events have been increasing in magnitude and, to a lesser degree, in frequency during the wet season beginning in 1979. Starting from 1950, we found an increase in rainfall at the transition zone between the low and intermediate elevations, partly reflected by the magnitude of extreme events in the northernmost NW Argentine provinces, whereas no trend signal was found for the same period at low elevations.

These observations partially agree with previous studies, showing changing extreme rainfall events for Argentina and other continental regions (Frei and Schär 2001; Krishnamurthy et al. 2009; Penalba and Robledo 2010; Skansi et al. 2013; Malik et al. 2016). In particular, Penalba and Robledo (2010) analyzed the trend of the frequency of rainy days and of events exceeding the 75th frequency distribution percentile in Argentina. These authors found a general positive signal for all seasons for the period 1961–2000, except for the austral winter (JJA). At continental scale, Skansi et al. (2013) reported increasing trends in heavy precipitation events for the period 1950–2010, accompanying a significant wetting and intensified rainfall. These findings are in agreement with our results at the mountain front and at high elevations, but not at low elevations, where we did not observe any significant trend signal.

The observed increase in rainfall, both in total amount and extreme-event intensity, is consistent with the findings by Hsu et al. (2011). These authors showed that total monsoon precipitation has had significant positive trends during the past 30 years related to an increase in global mean-surface temperatures. Carvalho and Cavalcanti (2016) observed that the reanalysis products (CFSR and NCEP/NCAR) indicate a progressive increase in low-level tropospheric temperatures over tropical South America during the monsoon season. This can potentially alter ocean-land differential heating affecting the monsoonal circulation and moisture transport from the tropics to the subtropics. In fact, enhanced monsoonal circulation could affect the strength of the SALLJ and/or the SACZ, which are the most important features controlling moisture advection in the subtropics and the precipitation systems affecting the southern Central Andes. Interestingly, our results suggest that mountain front and high-elevation areas in the southern Central Andes respond more readily to changes in large-scale circulation.

6 Conclusions

We analyzed rainfall variability and trend patterns in the southern Central Andes (70°–60°W, 16°–32°S) at different spatiotemporal scales. We based our analysis on daily rain-gauge observations (40 gauges) and two gridded datasets (CPC-uni, TRMM 3B42 V7). We defined a set of six climate indices, covering the entire rainfall-frequency distribution at annual and seasonal scales, for three different time periods: 1950–2014, 1979–2014, and 1998–2014. In particular, we analyzed magnitude and frequency trends of different rainfall events, from low-moderate (<50th percentile) to the extremes (>95th percentile), and the rate of change at annual and seasonal scales. We focused our analysis on the wet season from December to February (DJF), contributing at least 40 % to the annual total rainfall amount, but we furnish additional insights for both the entire year and the dry season. Our study distinguishes between three geographic areas characterized by pronounced topographic, environmental, and climatic differences. These are the low-elevation regions in the eastern part of the study area, the mountain front (intermediate elevation) bordering the Andean mountain chain immediately to the west, with elevations between 0.5 and 3 km, and the high-elevation areas (>3 km) farther west in the southern Andean Plateau. In the following, we summarize our key findings:

1. Station data for the period 1950–2014 show an increase of the annual total rainfall amount and wet days frequency at the transition zone between the low and intermediate elevations, accompanied by a trend characterized by a wetter wet season and, to a lesser degree, a drier dry season. For the period 1979–2014 rain-gauge measurements exhibit a significant trend at low elevations towards decreasing annual rainfall total amounts. Decreasing annual rainfall total amounts were also detected at low elevations with the CPC dataset for the period 1979–2014 and TRMM data for 1998–2014. At high elevations, both the CPC and TRMM datasets indicate that extensive areas on the arid southern Andean Plateau (Puna de Atacama) as well as at the mountain front (between 20° and 23°S and between 25° and 30°S) record increasing annual rainfall total amounts and, to a lesser degree, frequency of wet days. At seasonal scale, we observed for the dry season an even more pronounced trend towards drier conditions, whereas for the wet season extensive areas exhibited increasing trends in seasonal rainfall total amount on the Puna de Atacama Plateau. This supports previous findings of 'the wet get wetter, the dry get drier' mechanism.

2. Daily rainfall frequency distribution analysis often revealed small or no changes in median values of the wet days/hours magnitude, but a significant tendency towards either local intensification or attenuation in the 95th percentiles (extreme rainfall events). This observation holds true for all datasets and strongly impacts the trends of rainfall total amounts. For the period 1950–2014, rain-gauge measurements showed that for the wet season extreme (≥95th Prct) events have undergone a significant increase in magnitude, but not in frequency at the transition zone between the low and intermediate elevations as well as at high elevations in the northernmost NW Argentine Provinces. This accounts for most of the rate of change in the total amount, particularly at the transition zone between the low and intermediate-elevation areas of the southern Central Andes. Starting in 1979 at high elevations on the Puna de Atacama Plateau, all gridded datasets reveal large areas with increasing magnitude of extreme rainfall events during DJF.

3. Discrepancies between the results of the three datasets were found and are related to the magnitude of trends and spatial localization of minima/maxima trend values. This is particularly true for the high-elevation areas both for annual rainfall totals and extreme events. We ascribe such discrepancies to the limitation of the CPC dataset, characterized by relatively low spatial resolution and scarcity of rain-gauge measurements within the transition between the low and high elevations, as well as on the arid Puna de Atacama Plateau. Besides these discrepancies, the CPC and TRMM datasets showed similar rainfall patterns, both clearly recording opposite trends between low and high elevations. Analysis of CPC and TRMM datasets exhibited some important similarities with the results obtained from rain gauges. Although the rain-gauge measurements do not display a strong coherent pattern as observed in the gridded datasets, we detected indications pointing toward an increasing magnitude of extreme rainfall at the mountain front areas by the station dataset. We suggest that the spatial inconsistency of the trend pattern from the station dataset is the lack of coherent significant results obtained at high elevations. Hence, the station data only partly support the trend towards increasing amounts and frequencies on the Puna de Atacama Plateau as observed by the gridded CPC and TRMM dataset.

Appendix: Quantile regression

Quantile regression, which is often used in climate-related studies (e.g., Friederichs and Hense 2007; Sankarasubramanian and Lall 2003; Elsner et al. 2008; Bremnes 2004) is an extension of median regression based on estimating the value of the parameter vector β from the set of allowable vectors that minimizes the mean-loss function:

$$L_\tau(\beta, y) = \frac{1}{n} \sum_{i=1}^{n} p_\tau \left\{ y_i - \mu(x_i, \beta) \right\} \tag{1}$$

where y_i (i = 1, …, n) are the response values, μ is the estimate of the τ quantile, and x_i and β are the covariate vector (in our case the time) and parameter vector, respectively. The loss function is $p_\tau (\cdot)$, where:

$$p_\tau(z) = |z|\{\tau \cdot I(z > 0) + (1 - \tau) \cdot I(z < 0)\} \tag{2}$$

and $I(\cdot)$ is the indicator function, which is 1 when the argument is true and 0, if not. The loss function is non-negative taking a minimum value of zero only when z = 0. Given a series of samples with μ constant (intercept-only model), the resulting value of β (a scalar in this case) that minimizes the total loss function occurs only when μ is equal to the τ quantile of the response. If the model fits well, a plot of fitted versus actual values will show that τ percentage of observed values should be less than the fitted values, with 1 − τ percentage of the observed values greater than that of the fitted values (Yu et al. 2003). The total loss function is an unbiased sample estimate of the expected value of $p_\tau[Y − \mu(x \cdot \beta)]$, and the minimization over β is a consistent estimate of the minimization of this expected value. For the fit, we employ a linear model for the regression function of the form:

$$\mu = \beta_0 + \sum_{i=1}^{p} \beta_i \cdot x_i \tag{3}$$

where x_i is climate covariate i and there are p of them. Uncertainties associated with quantile regression coefficients at the 95 % confidence level were estimated applying boot-strapping techniques with 200 minimum numbers of iterations (Hahn 1995).

References

AghaKouchak A, Nasrollahi N (2010) Semi-parametric and parametric inference of extreme value models for rainfall data. Water Resour Manag 24:1229–1249. doi:10.1007/s11269-009-9493-3

Antolini G, Auteri L, Pavan V et al (2015) A daily high-resolution gridded climatic data set for Emilia-Romagna, Italy, during 1961–2010. Int J Climatol. doi:10.1002/joc.4473

Barros V, Castañeda ME, Doyle M (2000) Recent precipitation trends in Southern South America East of the Andes: an indication of climatic variability. South. Hemisph. Paleo- Neoclimates. pp 187–206

Barros V, Clarke R, Silva Dias P (2013) Climate Change in the La Plata Basin. doi:10.1038/474046a

Beniston M, Fox DG, Adhikary S et al (1996) Impacts of climate change on mountain regions. Second Assess. Rep. Intergov. Panel Clim. Chang. Cambridge University Press, pp 191–213

Berbery EH, Barros VR (2002) The hydrologic cycle of the La Plata basin in South America. J Hydrometeorol 3:630–645

Bianchi AR, Yañez CE (1992) Las precipitaciones en el Noroeste Argentino, Inst. Nac. Tecnol. Agropecu. Estac´ıon Exp

Boers N, Bookhagen B, Marwan N et al (2013) Complex networks identify spatial patterns of extreme rainfall events of the South American monsoon system. Geophys Res Lett 40:4386–4392. doi:10.1002/grl.50681

Boers N, Bookhagen B, Barbosa H et al (2014a) Prediction of extreme floods in the Central Andes by means of Complex Networks. Nat Commun. doi:10.1038/ncomms6199

Boers N, Donner RV, Bookhagen B, Kurths J (2014b) Complex network analysis helps to identify impacts of the El Niño Southern oscillation on moisture divergence in South America. Clim Dyn. doi:10.1007/s00382-014-2265-7

Boers N, Rheinwalt A, Bookhagen B et al (2014c) The South American rainfall dipole: a complex network analysis of extreme events. Geophys Res Lett 41:7397–7405. doi:10.1002/2014GL061829

Boers N, Bookhagen B, Marengo JA et al (2015a) Extreme rainfall of the South American monsoon system: a dataset comparison using complex networks. J Clim 28:1031–1056. doi:10.1175/JCLI-D-14-00340.1

Boers N, Bookhagen B, Marwan N, Kurths J (2015b) Spatiotemporal characteristics and synchronization of extreme rainfall in South America with focus on the Andes Mountain range. Clim Dyn. doi:10.1007/s00382-015-2601-6

Bombardi RJ, Carvalho LMV, Jones C (2013) Simulating the influence of the South Atlantic dipole on the South Atlantic convergence zone during neutral ENSO. Theor Appl Climatol. doi:10.1007/s00704-013-1056-0

Bookhagen B, Burbank DW (2010) Toward a complete Himalayan hydrological budget: spatiotemporal distribution of snowmelt and rainfall and their impact on river discharge. J Geophys Res 115:F03019. doi:10.1029/2009JF001426

Bookhagen B, Strecker MR (2008) Orographic barriers, high-resolution TRMM rainfall, and relief variations along the eastern Andes. Geophys Res Lett 35:L06403. doi:10.1029/2007GL032011

Bookhagen B, Strecker MR (2011) Modern Andean rainfall variation during ENSO cycles and its impact on the Amazon drainage basin. In: Hoorn C, Wesselingh FP (eds) Amaz Landsc. Species

Evol. A look into past. Blackwell Publishing, Hoboken, pp 223–241

Bookhagen B, Strecker MR (2012) Spatiotemporal trends in erosion rates across a pronounced rainfall gradient: examples from the southern Central Andes. Earth Planet Sci Lett 327–328:97–110. doi:10.1016/j.epsl.2012.02.005

Bremnes JB (2004) Probabilistic wind power forecasts using local quantile regression. Wind Energy 7:47–54. doi:10.1002/we.107

Cade B, Noon B (2003) A gentle introduction to quantile regression for ecologists. Front Ecol Environ 1:412–420

Caine N (1980) The rainfall intensity: duration control of shallow landslides and debris flows. Geogr Ann Ser A Phys Geogr 62:23–27. doi:10.2307/520449

Campetella CM, Vera CS (2002) The influence of the Andes mountains on the South American low-level flow. Geophys Res Lett 29:1826. doi:10.1029/2002GL015451

Carvalho LMV, Cavalcanti IFA (2016) The South American monsoon system (SAMS). In: Carvalho LMV, Jones C (eds) Monsoons and climate change. Springer, Berlin, pp 219–267

Carvalho LMV, Jones C (2016) The monsoons and climate change. Springer, Berlin

Carvalho LMV, Jones C, Liebmann B (2004) The South Atlantic convergence zone: intensity, form, persistence, and relationships with intraseasonal to interannual activity and extreme rainfall. J Clim 17:88–108

Carvalho LMV, Jones C, Silva AE et al (2011) The South American monsoon system and the 1970s climate transition. Int J Climatol 31:1248–1256. doi:10.1002/joc.2147

Carvalho LMV, Jones C, Posadas AND et al (2012) Precipitation characteristics of the South American monsoon system derived from multiple datasets. J Clim 25:4600–4620. doi:10.1175/JCLI-D-11-00335.1

Chen M, Shi W, Xie P et al (2008) Assessing objective techniques for gauge-based analyses of global daily precipitation. J Geophys Res Atmos 113:1–13. doi:10.1029/2007JD009132

Chen S, Hong Y, Gourley JJ et al (2013) Evaluation of the successive V6 and V7 TRMM multisatellite precipitation analysis over the Continental United States. Water Resour Res 49:8174–8186. doi:10.1002/2012WR012795

Cohen JCP, Silva Dias MAF, Nobre CA (1995) Environmental conditions associated with Amazonian squall lines: a case study. Mon Weather Rev 123:3163–3174

Condom T, Rau P, Espinoza JC (2011) Correction of TRMM 3B43 monthly precipitation data over the mountainous areas of Peru during the period 1998–2007. Hydrol Process 25:1924–1933. doi:10.1002/hyp.7949

da Silva A, de Carvalho L (2007) Large-scale index for South America Monsoon (LISAM). Atmos Sci Lett. doi:10.1002/asl

Dai A, Fung IY, Del Genio AD (1997) Surface observed global land precipitation variations during 1900-88. J Clim 10:2943–2962

Daly C (2006) Guidelines for assessing the suitability of spatial climate data sets. Int J Climatol 26:707–721. doi:10.1002/joc.1322

Daly C, Neilson RP, Phillips DL (1994) A statistical-topographic model for mapping climatological precipitation over mountainous terrain. J Appl Meteorol 33:140–158

de la Torre A, Pessano H, Hierro R et al (2015) The influence of topography on vertical velocity of air in relation to severe storms near the Southern Andes Mountains. Atmos Res 156:91–101. doi:10.1016/j.atmosres.2014.12.020

Skansi MM, Brunet M, Sigró J et al (2013) Warming and wetting signals emerging from analysis of changes in climate extreme indices over South America. Glob Planet Change 100:295–307. doi:10.1016/j.gloplacha.2012.11.004

Dee DP, Uppala SM, Simmons AJ et al (2011) The ERA-Interim reanalysis: configuration and performance of the data assimilation system. Q J R Meteorol Soc 137:553–597. doi:10.1002/qj.828

Durkee JD, Mote TL, Shepherd JM (2009) The contribution of mesoscale convective complexes to rainfall across subtropical South America. J Clim 22:4590–4605. doi:10.1175/2009JCLI2858.1

Elsner JB, Kossin JP, Jagger TH (2008) The increasing intensity of the strongest tropical cyclones. Nature 455:92–95. doi:10.1038/nature07234

Ensor LA, Robeson SM (2008) Statistical characteristics of daily precipitation: comparisons of gridded and point datasets. J Appl Meteorol Climatol 47:2468–2476. doi:10.1175/2008JAMC1757.1

Espinoza JC, Lengaigne M, Ronchail J, Janicot S (2012) Large-scale circulation patterns and related rainfall in the Amazon Basin: a neuronal networks approach. Clim Dyn 38:121–140. doi:10.1007/s00382-011-1010-8

Espinoza JC, Chavez S, Ronchail J et al (2015) Rainfall hotspots over the southern tropical Andes: spatial distribution, rainfall intensity, and relations with large-scale atmospheric circulation. Water Resour Res 6:446. doi:10.1002/2014WR016273

Frei C, Schär C (2001) Detection probability of trends in rare events: theory and application to heavy precipitation in the Alpine region. J Clim 14:1568–1584

Friederichs P, Hense A (2007) Statistical downscaling of extreme precipitation events using censored quantile regression. Mon Weather Rev 135:2365–2378. doi:10.1175/MWR3403.1

Gandu A, Geisler J (1991) A primitive equations model study of the effect of topography on the summer circulation over tropical South America. J Atmos Sci 48:1822–1836

Gandu AW, Silva Dias PL (1998) Impact of tropical heat sources on the South American tropospheric upper circulation and subsidence. J Geophys Res 103:6001. doi:10.1029/97JD03114

Garreaud R (2000) Cold air incursions over subtropical South America: mean structure and dynamics. Mon Weather Rev 128:2544–2559

Garreaud R, Aceituno P (2001) Interannual rainfall variability over the South American Altiplano. J Clim 14:2779–2789

Garreaud R, Vuille M, Clement AC (2003) The climate of the Altiplano: observed current conditions and mechanisms of past changes. Palaeogeogr Palaeoclimatol Palaeoecol 194:5–22. doi:10.1016/S0031-0182(03)00269-4

Garreaud RD, Molina A, Farias M (2010) Andean uplift, ocean cooling and Atacama hyperaridity: a climate modeling perspective. Earth Planet Sci Lett 292:39–50. doi:10.1016/j.epsl.2010.01.017

Giorgi F, Lionello P (2008) Climate change projections for the Mediterranean region. Glob Planet Change 63:90–104. doi:10.1016/j.gloplacha.2007.09.005

Giovannettone JP, Barros AP (2009) Probing regional orographic controls of precipitation and cloudiness in the central Andes using satellite data. J Hydrometeorol 10:167–182. doi:10.1175/2008JHM973.1

Gloor M, Brienen RJW, Galbraith D et al (2013) Intensification of the Amazon hydrological cycle over the last two decades. Geophys Res Lett 40:1729–1733. doi:10.1002/grl.50377

Gosset WS (1908) The Probable error of a mean. Biometrika 6:1–24

Goswami BN, Venugopal V, Sengupta D et al (2006) Increasing trend of extreme rain events over india in a warming environment. Science 314:1442–1445. doi:10.1126/science.1132027

Hahn J (1995) Cambridge University Press. Econ Theory 11:105–121

Halloy S (1982) Contribucíon al estudio de la zona de Huaca huasi, Cumbres Calchaquíes (Tucumán Argentina). Univ. Nac., Tucumán

Haylock M, Nicholls N (2000) Trends in extreme rainfall indices for an updated high quality data set for Australia, 1910–1998. Int J Climatol 20:1533–1541

Haylock MR, Peterson TC, Alves LM et al (2006) Trends in total and extreme South American rainfall in 1960–2000 and links with sea surface temperature. J Clim 19:1490–1512. doi:10.1175/JCLI3695.1

Heidinger H, Yarlequé C, Posadas A, Quiroz R (2012) TRMM rainfall correction over the Andean Plateau using wavelet multi-resolution analysis. Int J Remote Sens 33:4583–4602. doi:10.1080/01431161.2011.652315

Held IM, Soden BJ (2006) Robust responses of the hydrological cycle to global warming. J Clim 19:5686–5699. doi:10.1175/JCLI3990.1

Higgins RW, Shi W, Yarosh E, Joyce R (2000) Improved United States precipitation quality control system and analysis—Atlas No. 7

Holland PW, Welsch RE (1977) Robust regression using iteratively reweighted least-squares. Commun Stat Theory Methods 6:813–827. doi:10.1080/03610927708827533

Houston J (2006) The great Atacama flood of 2001 and its implications for Andean hydrology. Hydrol Process 20:591–610. doi:10.1002/hyp.5926

Hsu PC, Li T, Wang B (2011) Trends in global monsoon area and precipitation over the past 30 years. Geophys Res Lett 38:1–5. doi:10.1029/2011GL046893

Huber PJ (1981) Robust statistics. Wiley, New York

Huffman GJ, Bolvin DT, Nelkin EJ et al (2007) The TRMM multisatellite precipitation analysis (TMPA): quasi-global, multiyear, combined-sensor precipitation estimates at fine scales. J Hydrometeorol 8:38–55. doi:10.1175/JHM560.1

Insel N, Poulsen C, Ehlers T (2010) Influence of the Andes Mountains on South American moisture transport, convection, and precipitation. Clim Dyn 35:1477–1492. doi:10.1007/s00382-009-0637-1

Isotta FA, Frei C, Weilguni V et al (2014) The climate of daily precipitation in the Alps: development and analysis of a high-resolution grid dataset from pan-Alpine rain-gauge data. Int J Climatol 34:1657–1675. doi:10.1002/joc.3794

Jacques-Coper M, Garreaud RD (2015) Characterization of the 1970s climate shift in South America. Int J Climatol 35:2164–2179. doi:10.1002/joc.4120

Jones C, Carvalho LMV (2014) Sensitivity to Madden-Julian oscillation variations on heavy precipitation over the contiguous United States. Atmos Res 147–148:10–26. doi:10.1016/j.atmosres.2014.05.002

Jones C, Carvalho LMV, Liebmann B (2012) Forecast skill of the South American monsoon system. J Clim 25:1883–1889. doi:10.1175/JCLI-D-11-00586.1

Kendon E, Roberts N, Fowler H (2014) Heavier summer downpours with climate change revealed by weather forecast resolution model. Nat Clim Change 4:1–7. doi:10.1038/NCLIMATE2258

Koenker R, Bassett G Jr (1978) Regression quantiles. Econometrica 46:33–50. doi:10.2307/1913643

Krishnamurthy CKB, Lall U, Kwon H-H (2009) Changing frequency and intensity of rainfall extremes over India from 1951 to 2003. J Clim 22:4737–4746. doi:10.1175/2009JCLI2896.1

Kummerow C, Barnes W, Kozu T et al (1998) The tropical rainfall measuring mission (TRMM) sensor package. J Atmos Ocean Technol 15:809–817

Kummerow C, Simpson J, Thiele O et al (2000) The status of the tropical rainfall measuring mission (TRMM) after two years in orbit. J Appl Meteorol 39:1965–1982

Lavado Casimiro WS, Labat D, Ronchail J et al (2013) Trends in rainfall and temperature in the Peruvian Amazon–Andes basin over the last 40 years (1965–2007). Hydrol Process 27:2944–2957. doi:10.1002/hyp.9418

Liebmann B, Allured D (2005) Daily precipitation grids for South America. Bull Am Meteorol Soc 86:1567–1570. doi:10.1175/BAMS-86-11-1567

Longobardi A, Villani P (2009) Trend analysis of annual and seasonal rainfall time series in the Mediterranean area. Int J Climatol. doi:10.1002/joc.2001

Madden RA, Julian PR (1971) Detection of a 40–50 day oscillation in the zonal wind in the tropical Pacific. J Atmos Sci 28:702–708

Maddox RA, Chappell CF, Hoxit LR (1979) Synoptic and mesoscale aspects of flash flood events. Bull Am Meteorol Soc 60:115–123

Malik N, Bookhagen B, Marwan N, Kurths J (2011) Analysis of spatial and temporal extreme monsoonal rainfall over South Asia using complex networks. Clim Dyn 39:971–987. doi:10.1007/s00382-011-1156-4

Malik N, Bookhagen B, Mucha PJ (2016) Spatiotemporal patterns and trends of Indian monsoonal rainfall extremes. Geophys Res Lett. doi:10.1002/2016GL067841

Mantua N, Hare S (2002) The Pacific decadal oscillation. J Oceanogr 58:35–44

Marengo JA (2004) Interdecadal variability and trends of rainfall across the Amazon basin. Theor Appl Climatol 78:79–96. doi:10.1007/s00704-004-0045-8

Marengo JA, Liebmann B, Grimm AM et al (2012) Recent developments on the South American monsoon system. Int J Climatol 32:1–21. doi:10.1002/joc.2254

Minetti JL, Vargas WM (1998) Trends and jumps in annual precipitation in South America, south of the 15°S. Atmosfera 11:205–211

Minvielle M, Garreaud RD (2011) Projecting rainfall changes over the South American Altiplano. J Clim 24:4577–4583. doi:10.1175/JCLI-D-11-00051.1

Nerini D, Zulkafli Z, Wang L-P et al (2015) A comparative analysis of TRMM–rain gauge data merging techniques at the daily time scale for distributed rainfall–runoff modeling applications. J Hydrometeorol 16:2153–2168. doi:10.1175/JHM-D-14-0197.1

Papalexiou SM, Koutsoyiannis D (2013) Battle of extreme value distributions: a global survey on extreme daily rainfall. Water Resour Res 49:187–201. doi:10.1029/2012WR012557

Penalba OC, Robledo FA (2010) Spatial and temporal variability of the frequency of extreme daily rainfall regime in the La Plata Basin during the 20th century. Clim Change 98:531–550. doi:10.1007/s10584-009-9744-6

Pepin N, Bradley RS, Diaz HF et al (2015) Elevation-dependent warming in mountain regions of the world. Nat Clim Change 5:424–430. doi:10.1038/nclimate2563

Rajczak J, Pall P, Schär C (2013) Projections of extreme precipitation events in regional climate simulations for Europe and the Alpine Region. J Geophys Res Atmos 118:3610–3626. doi:10.1002/jgrd.502972013

Rao VB, Franchito SH, Santo CME, Gan MA (2015) An update on the rainfall characteristics of Brazil: seasonal variations and trends in 1979–2011. Int J Climatol. doi:10.1002/joc.4345

Rienecker MM, Suarez MJ, Gelaro R et al (2011) MERRA: nASA's modern-era retrospective analysis for research and applications. J Clim 24:3624–3648. doi:10.1175/JCLI-D-11-00015.1

Robledo FA, Vera C, Penalba OC (2015) Influence of the large-scale climate variability on daily rainfall extremes over Argentina. Int J Climatol. doi:10.1002/joc.4359

Rodda JC (2011) Guide to hydrological practices. Hydrol Sci J 56:196–197. doi:10.1080/02626667.2011.546602

Rohmeder W (1943) Observaciones meterológicas en la región encumbrada de las Sierras de Famatina y del Aconquija (republica Argentina). An Soc Cient Arg 136:97–124

Rohrmann A, Strecker MR, Bookhagen B et al (2014) Can stable isotopes ride out the storms? The role of convection for water isotopes in models, records, and paleoaltimetry studies in the central Andes. Earth Planet Sci Lett 407:187–195. doi:10.1016/j.epsl.2014.09.021

Romatschke U, Houze RA (2010) Extreme summer convection in South America. J Clim 23:3761–3791. doi:10.1175/2010JCLI3465.1

Romatschke U, Houze RA (2013) Characteristics of precipitating convective systems accounting for the summer rainfall of tropical and subtropical South America. J Hydrometeorol. doi:10.1175/JHM-D-12-060.1

Romatschke U, Medina S, Houze RA (2010) Regional, seasonal, and diurnal variations of extreme convection in the South Asian region. J Clim 23:419–439. doi:10.1175/2009JCLI3140.1

Ruscica RC, Sörensson AA, Menéndez CG (2014) Hydrological links in Southeastern South America: soil moisture memory and coupling within a hot spot. Int J Climatol 3653:3641–3653. doi:10.1002/joc.3930

Rusticucci M, Penalba O (2000) Interdecadal changes in the precipitation seasonal cycle over Southern South America and their relationship with surface temperature. Clim Res 16:1–15. doi:10.3354/cr016001

Salio P, Nicolini M, Saulo AC (2002) Chaco low-level jet events characterization during the austral summer season. J Geophys Res Atmos 107:4816. doi:10.1029/2001JD001315

Sankarasubramanian A, Lall U (2003) Flood quantiles in a changing climate: seasonal forecasts and causal relations. Water Resour Res 39:1–12. doi:10.1029/2002WR001593

Seluchi ME, Marengo JA (2000) Tropical—midlatitude exchange of air masses during summer and winter in South America: climatic aspects. Int J Climatol 1190:1167–1190

Sen Roy S, Balling RC (2004) Trends in extreme daily precipitation indices in India. Int J Climatol 24:457–466. doi:10.1002/joc.995

Sen Z, Habib Z (2000) Spatial analysis of monthly precipitation in Turkey. Theor Appl Climatol 67:81–96. doi:10.1007/s007040070017

Seneviratne SI, Nicholls N, Easterling D, et al. (2012) Changes in climate extremes and their impacts on the natural physical environment. In: Field CB, Barros V, Stocker TF, et al. (eds) Manag. Risks Extrem. Events Disasters to Adv. Clim. Chang. Adapt. A Spec. Rep. Work. Groups I II Intergov. Panel Clim. Chang. Cambridge, UK, and New York, NY, USA, pp 109–230

Serinaldi F, Kilsby CG (2014) Rainfall extremes: toward reconciliation after the battle of distributions. Water Resour Res 50:336–352. doi:10.1002/2013WR014211

Sillmann J, Kharin VV, Zwiers FW et al (2013) Climate extremes indices in the CMIP5 multimodel ensemble: part 2. Future climate projections. J Geophys Res Atmos 118:2473–2493. doi:10.1002/jgrd.50188

Silva VBS, Kousky VE, Shi W, Higgins RW (2007) An improved gridded historical daily precipitation analysis for Brazil. J Hydrometeorol 8:847–861. doi:10.1175/JHM598.1

Tank AK, Zwiers FW, Zhang X (2009) Guidelines on analysis of extremes in a changing climate in support of informed decisions for adaptation, WCDMP-No. 72

Thibeault JM, Seth A, Garcia M (2010) Changing climate in the Bolivian Altiplano: CMIP3 projections for temperature and precipitation extremes. J Geophys Res Atmos 115:1–18. doi:10.1029/2009JD012718

Thibeault J, Seth A, Wang G (2012) Mechanisms of summertime precipitation variability in the bolivian altiplano: present and future. Int J Climatol 32:2033–2041. doi:10.1002/joc.2424

Trenberth KE, Dai A, Rasmussen RM, Parsons DB (2003) The changing character of precipitation. Bull Am Meteorol Soc 84:1205–1217. doi:10.1175/BAMS-84-9-1205

Tucci CEM, Clarke RT (1998) Environmental issues in the la Plata basin. Int J Water Resour Dev 14:157–173. doi:10.1080/07900629849376

Urrutia R, Vuille M (2009) Climate change projections for the tropical Andes using a regional climate model: temperature and precipitation simulations for the end of the 21st century. J Geophys Res 114:D02108. doi:10.1029/2008JD011021

Vera C, Higgins W, Amador J et al (2006) Toward a unified view of the American monsoon systems. J Clim 19:4977–5000. doi:10.1175/JCLI3896.1

Vuille M, Keimig F (2004) Interannual variability of summertime convective cloudiness and precipitation in the Central Andes derived from ISCCP-B3 data. J Clim 17:3334–3348

Vuille M, Bradley RS, Keimig F (2000) Climate variability in the Andes of Ecuador and its relation to tropical Pacific and Atlantic sea surface temperature anomalies. J Clim 13:2520–2535. doi:10.1175/1520-0442(2000)013<2520:CVITAO>2.0.CO;2

Vuille M, Franquist E, Garreaud R et al (2015) Impact of the global warming hiatus on Andean temperature. J Geophys Res Atmos 120:3745–3757. doi:10.1002/2015JD023126

White GF, Haas JE (1975) Assessment of research on natural hazard. MIT Press, Cambridge

WMO (2008) Guide to hydrological practices, 6th edn. WMO, Geneva. doi:10.1080/02626667.2011.546602

World Meteorological Organization (2011) Guide to climatological practices WMO-No. 100, WMO. WMO, Geneva

Wulf H, Bookhagen B, Scherler D (2012) Climatic and geologic controls on suspended sediment flux in the Sutlej River Valley, western Himalaya. Hydrol Earth Syst Sci 16:2193–2217. doi:10.5194/hess-16-2193-2012

Wulf H, Bookhagen B, Scherler D (2016) Differentiating between rain, snow, and glacier contributions to river discharge in the western Himalaya using remote-sensing data and distributed hydrological modeling. Adv Water Resour 88:152–169. doi:10.1016/j.advwatres.2015.12.004

Xie P, Chen M, Yang S et al (2007) A gauge-based analysis of daily precipitation over East Asia. J Hydrometeorol 8:607–626. doi:10.1175/JHM583.1

Xue X, Hong Y, Limaye AS et al (2013) Statistical and hydrological evaluation of TRMM-based multi-satellite precipitation analysis over the Wangchu Basin of Bhutan: are the latest satellite precipitation products 3B42V7 ready for use in ungauged basins? J Hydrol 499:91–99. doi:10.1016/j.jhydrol.2013.06.042

Yu K, Lu Z, Stander J (2003) Quantile regression: applications and current research areas. J R Stat Soc Ser D Stat 52:331–350. doi:10.1111/1467-9884.00363

Yue S, Pilon P (2004) A comparison of the power of the t test, Mann-Kendall and bootstrap tests for trend detection. Hydrol Sci J 49:21–37. doi:10.1623/hysj.49.1.21.53996

Zhou J, Lau K-M (1998) Does a monsoon climate exist over South America? J Clim 11:1020–1040

Zulkafli Z, Buytaert W, Onof C et al (2014) A comparative performance analysis of TRMM 3B42 (TMPA) versions 6 and 7 for hydrological applications over Andean-Amazon river basins. J Hydrometeorol 15:581–592. doi:10.1175/JHM-D-13-094.1